Mechanical properties of (steel-reinforced) resins used in injected bolted connections

Nijgh, Martin; Xin, Haohui; Veljkovic, Milan

Publication date
2019

Document Version
Final published version

Published in
Proceedings of the 22nd International Conference on Composite Materials

MECHANICAL PROPERTIES OF (STEEL-REINFORCED) RESINS USED IN INJECTED BOLTED CONNECTIONS

Martin P. Nijgh[1], Haohui Xin[1] and Milan Veljkovic[1]

[1] Delft University of Technology, Faculty of Civil Engineering & Geosciences, Delft, The Netherlands

Keywords: Steel-reinforced resin, Epoxy resin, Homogenization, Finite element simulation

ABSTRACT

This paper illustrates the most recent developments in the field of injected bolted connections. A novel injection material, steel-reinforced resin, is used to enhance stiffness of resin-injected bolted shear connections. The main goal is to achieve the slip resistance connection in a clearance holes without pre-tensioning of bolts. Steel-reinforced resins consist of spherical steel particles embedded in an epoxy resin matrix. Steel-reinforced resins are characterized by a higher Young's Modulus compared to the bare epoxy resin. Numerical and analytical prediction methods for the quasi-static mechanical behaviour of steel-reinforced resins are presented and validated based on small-scale compression tests. The design of a tailor-made test setup, the simple pin connection, is presented. This setup allows for investigation of a generic behaviour of steel-reinforced resins subject to cyclic loading in confined conditions. Preliminary results obtained with the simple pin connection specimens are shown and improvements of the setup, specimens and process are discussed. An overview of potential applications focusing on easy and fast execution, dissembling and reuse of steel and steel/concrete structures is presented.

1 INTRODUCTION

Injection bolts are a standardized type of bolts [1] used in injected bolted connections (IBCs). IBCs are connections of which the bolt-to-hole clearance is injected with an epoxy resin. The cured epoxy resin mitigates the displacement (slip) of the connected members, and therefore IBCs are classified as slip-resistant. Originally [2] [3], IBCs have been used to replace faulty riveted steel-to-steel connections in railway bridges because (i) riveting is no longer common and (ii) the actual slip factor of the faying surfaces cannot be determined. The most commonly used combination of epoxy resin and hardener in IBCs is RenGel SW404 + HY2404/HY5159, being the only certified epoxy resin system to be used in Dutch infrastructural works [4]. Compression, tension and shear tests on this epoxy resin system with hardener HY404 (the predecessor of HY2404) have been carried out by Wedekamper [5].

A novel application of IBCs is in in the field of demountable and reusable composite steel-concrete composite flooring systems, as studied by Nijgh et. al [6]. In their work, composite action is obtained by bolted shear connectors embedded in the concrete deck, which are connected to the steel beam flange. To ensure fast execution and easy demountability of the floor system with relatively large prefabricated decks (2,7 m x 8 m), sufficient allowance must be made for the fabrication and execution tolerances. The allowance is considered by opting for oversize holes in the beam flange. The contradictory requirement of the composite floor system, namely oversize holes in construction stage and composite interaction in the final stage, is solved by injecting the bolt-to-hole clearance with epoxy resin [6]. It was found that all shear connectors contribute instantaneously and simultaneously due to the epoxy resin injection [6].

The goal of this paper is to present a novel injection material, steel-reinforced resin, with a higher Young's Modulus compared to normal epoxy resins, and to assess its mechanical behaviour under static loading and to illustrate methods to determine its behaviour under cyclic loads. Applications of the novel injection material include both steel-to-steel and hybrid connections in buildings and infrastructure. Application of steel-reinforced resin and resin-injected connections reduces the need for pretensioning of bolts to achieve a stiff shear connection.

2 DEVELOPMENT OF STEEL-REINFORCED RESIN

The effects of oversize holes on the connections stiffness of steel-to-steel IBCs with M20 bolts was investigated by Nijgh [7], who carried out double lap shear tests on IBCs with varying dimensions of the bolt holes in the centre plates. It was found that the stiffness of the IBC decreased for increasing bolt hole sizes. To mitigate the decrease of the connection stiffness, a novel material was developed that consists of steel spherical particles (shot) which are embedded in the original epoxy resin matrix. This novel material is referred to as steel-reinforced resin, and typically contains 60% of steel particles and 40% of resin (in volume). Figure 1 shows a cross-section of a steel-reinforced resin infill taken from an IBC. Steel shot is a product used in the grit blasting industry and can be used in IBCs as reinforcing material because of its abundance, low costs, and high mechanical properties (as steel). Several sizes of steel shot are on the market, ranging from a diameter of tenths of a mm to several mm.

The stiffness of the IBCs cf. EN Annex G/K of EN 1090-2 [8] tested by Nijgh [7] with epoxy resin and steel-reinforced resin is shown in Figure 2. The results clearly show that using steel-reinforced resin allows for the use of significantly oversize holes without compromising on the connection stiffness compared to a IBC with a standard hole size. Further experiments with steel-reinforced resin specimens are planned to quantify benefits of steel-reinforced resin for other bolt hole diameters.

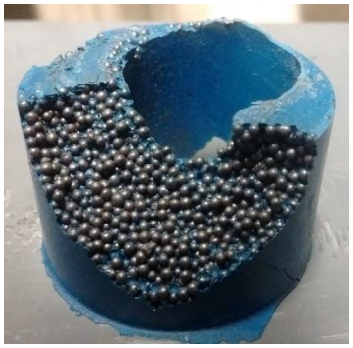

Figure 1: Cross-section of steel-reinforced resin.

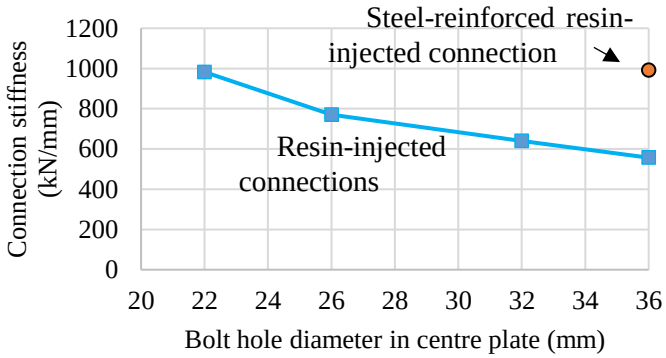

Figure 2: Stiffness of IBCs with significantly oversize bolt holes in centre plates of a double lap shear connection with M20 bolts, for resin and steel-reinforced resin as injection material [7].

3 QUASI-STATIC UNIAXIAL COMPRESSION TESTS

The static mechanical properties of steel-reinforced resin are determined using quasi-static uniaxial compression tests on cylindrical specimen with a length of 50 mm and a diameter of 26 mm. The epoxy resin system RenGel SW404 + HY2404 is used in combination with steel shot with a nominal diameter of 1.0 mm. The mechanical properties of the resin are also tested, using the same geometry, to serve as input in homogenization methods. The experimental set-up is illustrated in Figure 3. The load is applied using a stroke-controlled regime at a speed of 0.01 mm/s. Two Ono Sokki GS-551 linear gauge sensors with a range of 0.001 - 5 mm were used to measure the axial deformation of the specimen. The typical failure modes of the resin and steel-reinforced resin specimen are illustrated in Figure 4.

A combination of computational and analytical homogenization methods are used to predict the quasi-static material properties of the steel-reinforced resin based on the material properties of the resin (as separately tested) and the reinforcing steel particles.

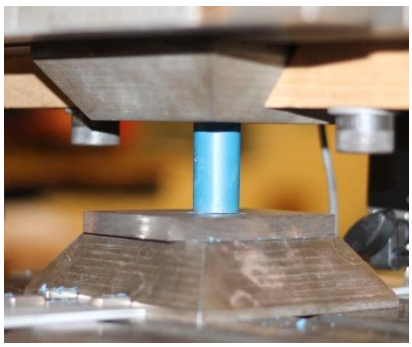

Figure 3: Cylindrical resin specimen subject to uniaxial compression.

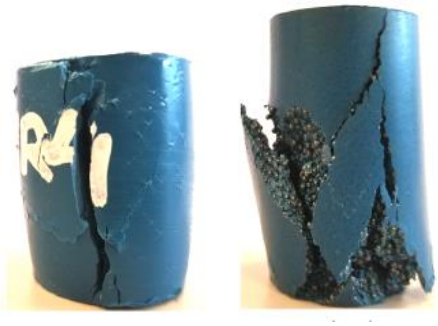

Figure 4: Typical failure modes for resin (left) and steel-reinforced resin (right) specimens.

3.1 Analytical homogenization method

The elastic and plastic response of the steel-reinforced resin can be modelled using an analytical approach by assuming the spatial distribution of the reinforcing steel particles to be known [9]. An example of a spatial distribution is the body-centered cubic packing as illustrated in Figure 5. The response of the steel-reinforced resin can then be determined by discretizing the volume and regarding each discretized element as a spring element with steel and resin components in series, with the respective individual spring stiffnesses given as

$$k_{\mathrm{s}}(x_i, y_j) = \frac{E_{\mathrm{s}} \cdot \frac{1}{n^2}}{h_{\mathrm{s}}(x_i, y_j)} \quad ; \quad k_{\mathrm{r}}(x_i, y_j) = \frac{E_{\mathrm{r}} \cdot \frac{1}{n^2}}{h_{\mathrm{r}}(x_i, y_j)}. \tag{1}$$

The definition of the variables in Eq. (1) is presented in Figure 5. The equivalent spring stiffness of these two serial springs can be determined by Eq. (2). The Young's Modulus of the steel-reinforced resin can be computed by summing the equivalent spring stiffness of all n^2 elements, as expressed through Eq. (3).

$$k_{\mathrm{eq}}(x_i, y_j) = \frac{k_{\mathrm{r}}(x_i, y_j) \cdot k_{\mathrm{s}}(x_i, y_j)}{k_{\mathrm{r}}(x_i, y_j) + k_{\mathrm{s}}(x_i, y_j)}. \tag{2}$$

$$E_{\mathrm{s+r}} = \sum_{j=1}^{n} \sum_{i=1}^{n} k_{\mathrm{eq}}(x_i, y_j). \tag{3}$$

This approach is a discretized version of the Reuss model [10]. Non-linear material behavior can be modelled through a damage model. In this case an iterative procedure is required to determine the stress-strain curve of the steel-reinforced resin. Iteration is carried out until the difference between the applied deformation u_0 and actual deformation $u_r(x_i,y_j)+ u_s(x_i,y_j)$ is sufficiently small, see Eq. (4).

$$\left| u_0 - \left[u_{\mathrm{r}}(x_i, y_j) + u_{\mathrm{s}}(x_i, y_j) \right] \right| < \left| \Delta u_{\max} \right|. \tag{4}$$

The spatial distribution of the reinforcing steel particles is proven to be accurately represented by a body centered cubic packing within the unit cell (see Figure 5). The difference between the results obtained using a body centered cubic packing and a random distribution of spheres in the unit cell (generated through computational simulation of sphere dropping and rolling) in terms of Young's Modulus is only 1%.

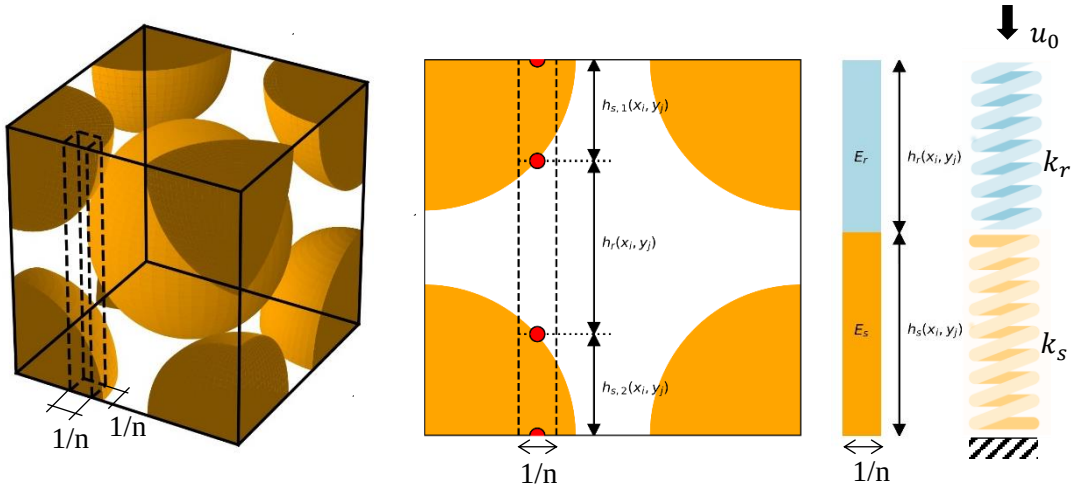

Figure 5: Left: Body-centered cubic arrangement of reinforcing steel spheres, indicating a discrete element with size 1 x 1/n x 1/n within the unit cell. Middle: cross-sectional view. Right: conversion of the discrete element into an equivalent spring.

3.2 Numerical homogenization method

The manufacturing process of steel reinforced resin makes it difficult to create tensile coupon specimens to obtain tensile behavior experimentally, due to the relatively large injection length in combination with a relatively high resin viscosity. The computational homogenization method provides an alternative way to obtain the tensile and shear behavior numerically after validating the multiscale model with compressive test results. The link between micro-scale and macro-scale behaviour is established based on Hill-Mandel computational homogenization method. The macro-scale Cauchy stress σ_{ij} is obtained by averaging the microscale Cauchy stress, $\tilde{\sigma}_{ij}$, in the unit cell domain [11], expressed as

$$\sigma_{ij} = \frac{1}{|\Theta|}\int_{\Theta} \tilde{\sigma}_{ij} d\Theta, \tag{5}$$

in which Θ is the domain of the unit cell. The unit cell problem can be solved for the leading order translation-free micro-scale displacement. The periodic boundary conditions [7] in the unit cell domain are implemented by so-called 'mixed boundary conditions' through constraint equations [11] [12], expressed through Eqs. (6)-(7), in which N_j^{Θ} is the unit normal to the unit cell boundary $\delta\Theta_y$.

$$\int_{\partial\Theta_Y} \left(u_i^f\left(x,y\right) - \varepsilon_{ik}^c y_k\right) N_j^{\Theta} d\gamma_Y = 0. \tag{6}$$

$$\left|u_i^f\left(x,y\right) - \varepsilon_{ik}^c y_k\right| N_j^{\Theta} \le Tol. \tag{7}$$

A 2D unit cell was considered in the homogenization process. The detailed parameters of the computational homogenization simulation can be found in ref. [13]. Based on the homogenization simulation a Drucker-Prager material model of the (steel-reinforced) resin was derived that can be used to simulate the compression behaviour of the (steel-reinforced) resin.

3.3 Results and discussion

The averaged stress-strain curves of the resin and steel-reinforced specimen under uniaxial compression are presented in Figure 6 including the results obtained by the analytical and numerical prediction methods. A good agreement is observed between both modelling methods and the experimental results, indicating the successful application of analytical and computational homogenization methods.

The Young's Modulus of the steel-reinforced resin is 2.8 times (15.7 GPa) that of the resin (5.64

GPa). The ductility of the resin is larger (20%) compared to that of the steel-reinforced resin (1.5%), but ductility is not an issue under confined conditions (such as in a bolted connection) because the confinement prevents the uniaxial failure modes from arising. Reference is made to refs. [9] [13] for the performance of the (steel-reinforced) resin under confined conditions.

The high Young's Modulus of steel-reinforced resin leads to smaller initial relative displacements in resin-injected bolted connections, which leads to higher admissible load levels for a given displacement criterion. The steel-reinforced resin contains approximately 60% of solid steel particles, inert to time-dependent deformation compared to the resin matrix, and therefore the response to creep and cyclic loading of the steel-reinforced resin is expected to be superior to that of only the resin matrix.

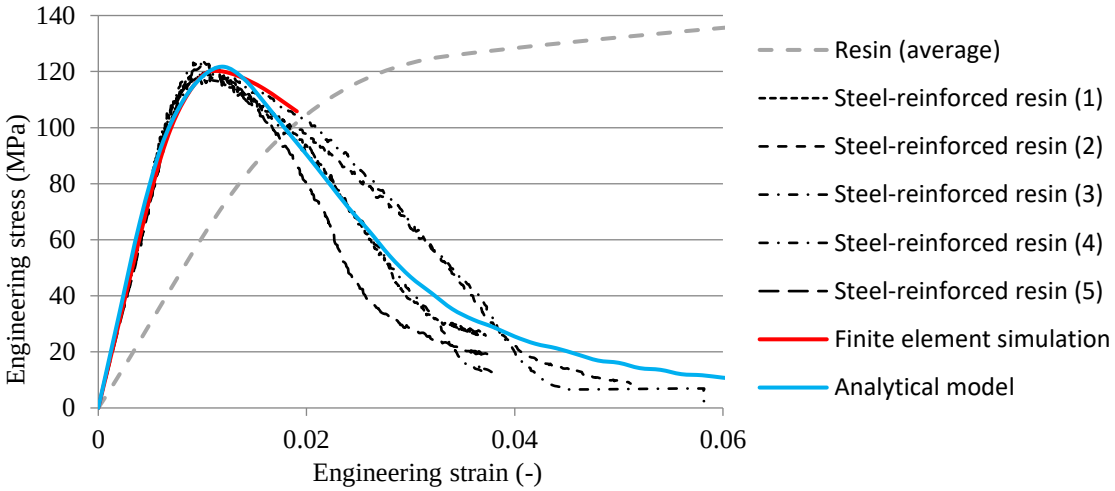

Figure 6: Stress-strain curve of the steel-reinforced resin showing experimental, analytical and numerical results.

4 TAILOR-MADE TEST SETUP FOR CYCLIC LOADING

The mechanical properties of the resin and steel-reinforced resin deteriorate with time, for instance due to repetitive (cyclic) loading and due to creep effects. The reduction in the mechanical properties results in decreased connection stiffness, which should be avoided in case of slip-resistant connections. In case of non-slip-critical connections, for instance shear connections that limit the deflection of statically loaded composite beams, the degradation of material properties may cause the beam to exceed serviceability limit state requirements.

A tailor-made test setup has been designed to determine the effects of sustained and cyclic loading on the mechanical properties of the (steel-reinforced) resin under in-use conditions and the subsequent effect of that on the stiffness of the injected bolted connection. The in-use conditions do not only refer to the confinement conditions, but also to the specimen geometry and the actual stress paths within the material. Typically, a double lap shear test is carried out for this purpose as prescribed in Annex G/K of EN 1090-2 [8], see Figure 7a.

The proposed test setup, see Figure 7b, is similar to the double lap shear tests. The bolts of the double lap shear connection are represented by a threaded pin in the proposed setup, which is referred to as the simple pin connection. This design change prevents the fatigue failure mode due to shear of the bolt as well as the influence of any deformation of the bolts. The main reason for the using a threaded pin is that fully threaded bolts are used in the demountable shear connector system used in demountable and reusable steel-concrete composite floor systems [6]. The threaded pin is placed in the most unfavourable position with respect to potential slip to obtain the worst-case scenario. The (steel-reinforced) resin is confined by the steel around the bolt hole and the two side plates. The resin and steel-reinforced resin are injected through Perspex cover plates, which provide visual control of the injection process. After curing of the resin, the Perspex cover plates are replaced by steel ones.

Numerical verification of the proposed setup and preliminary test results on simple pin connections subject to cyclic loading are presented in the next sections.

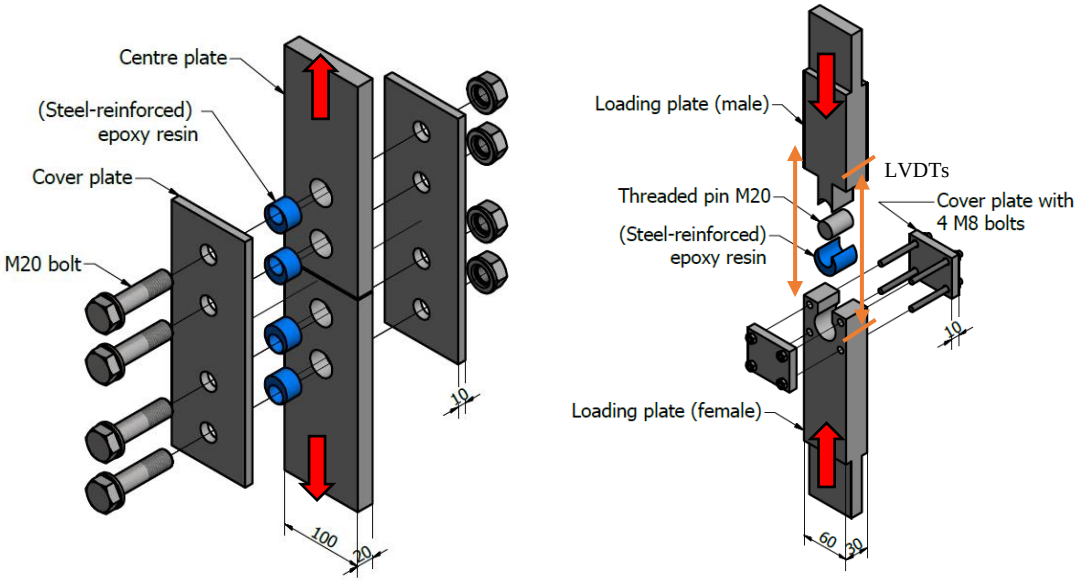

Figure 7: Left: Double-lap shear test cf. EN 1090-2 Annex G/K [8]. Right: Overview of tailor-made test setup (simple pin connection) used in the cyclic tests.

4.1 Numerical verification of test set-up

Numerical analysis is used to prove that the bearing stress distribution in case of the simple pin connection is equivalent to the bearing stress distribution for a double lap shear connection cf. Annex G/K of EN 1090-2 [8]. An elastic-plastic stress-strain for the steel plates is used with a yield strength of 355 MPa, whereas a non-linear material model for the (steel-reinforced) resin is taken from ref. [13]. A friction coefficient of 0.20 is assumed for both models. ABAQUS/Standard is used to carry out the analyses with the geometry specified in Figure 7.

Figure 8a illustrates the longitudinal bearing stress distribution in the resin along the pin/bolt perimeter for a force corresponding to a nominal bearing stress of 200 MPa (see Eq. (8)) for a specimen with an M20 pin or bolt positioned in the most negative location in a Ø26 mm hole. This nominal bearing stress is considered to be the limit for static applications in normal-clearance connections. The maximum longitudinal stress in the resin for the simple pin connection is 6% higher than in case of a double lap shear connection. This is an indicator that part of the force within the double lap shear connection is transferred by friction. If the effect of friction is corrected for by considering that all force is transferred by bearing (black dashed lines in Figure 8a) the difference between the two setups in terms of maximum longitudinal bearing stress is only 2%. It should be noted that in both FE analyses the threads of the pin and bolt have been ignored.

Figure 8b shows the bearing stress along the pin/bolt length. Again, a small and similar difference between the double lap shear connection and the simple pin connection is observed, which is attributed to frictional effects. For both setups, the bearing stress is approximately constant over the pin/bolt length. This indicates that the effects of bolt bending are insignificant in case of the double lap shear connection with the standard l/d (clamping length over bolt diameter) ratio of 2, which is in line with the EN 1993-1-8 [1] statement that a uniform bearing stress distributions may be expected for l/d ratios smaller than 3. In future studies, the effect of the threads on the connection behaviour will be investigated.

It can be concluded that the simple pin connection is theoretically correct to determine the deterioration of the mechanical properties of the connection under the same conditions as in the standardized double lap shear connection of Annex G/K of EN 1090-2 [8]. For large l/d ratios additional verification may be necessary.

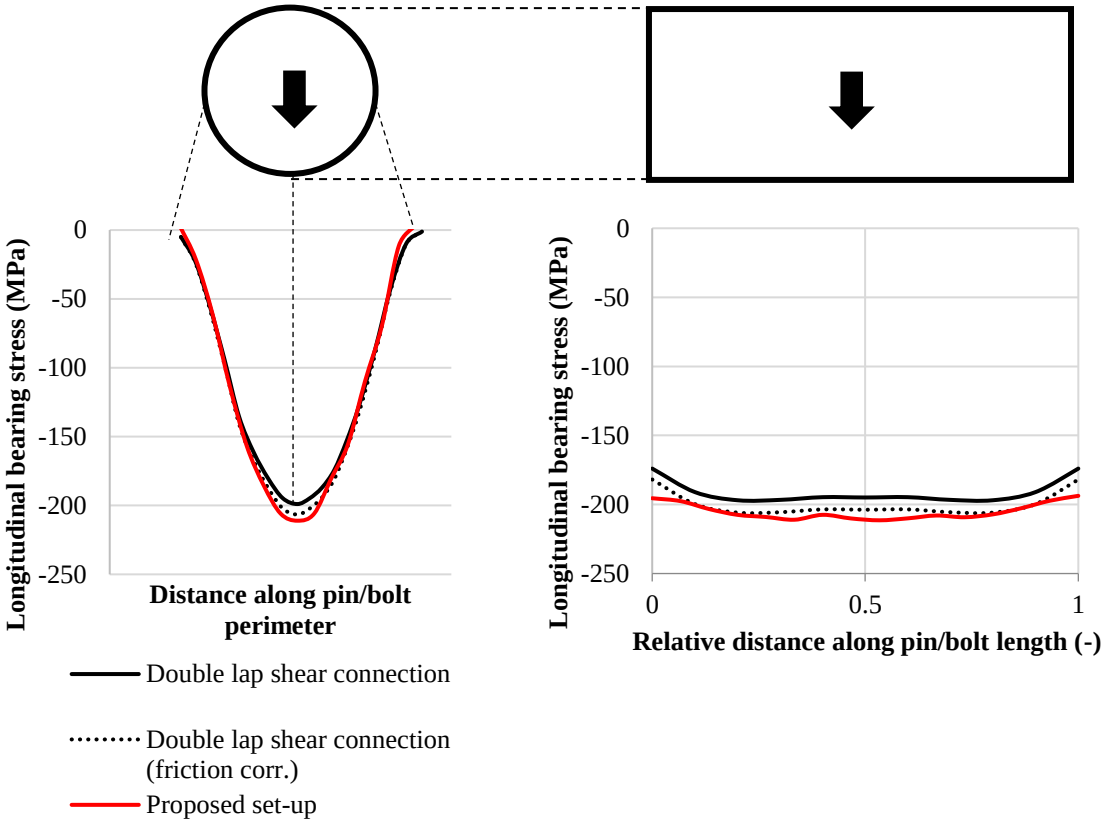

Figure 8: Longitudinal bearing stress distribution along the pin/bolt perimeter (left) and length (right).

4.2 Preliminary results of simple pin connections subject to cyclic loading

Preliminary tests using the simple pin connection setup with specimens subjected to cyclic loading have been carried out. The preliminary tests are part of a larger experimental programme, see Table 1, in which several bolt-to-hole clearances and applied stress levels are considered for resin and steel-reinforced resin injected specimens. The applied stress level is defined as a nominal bearing stress, denoted as

$$\sigma = \frac{F}{d_b t}, \tag{8}$$

in which F is the force applied by the actuator, d_b is the pin diameter (20 mm) and t is the plate thickness (30 mm).

The relative displacement between the upper and lower loading plates is registered using two LVDTs at the locations indicated in Figure 7b. The average of the LVDTs is used to assess the deformation of the specimen. Prior to the cyclic loading, the specimens are loaded by 25 quasi-static loading cycles at a speed of 0.05 Hz to determine the initial stiffness of the connection. Thereafter a cyclic load is applied at a speed of 5 Hz, following the ASTM recommendations for uniaxial fatigue loading [14]. It should be noted that, although the load itself is uniaxial, a multi-axial stress state exists in the resin layer due to confinement effects.

The preliminary tests have revealed the sensitivity of the setup to air inclusions within the specimens, see Figure 9, which are especially pronounced for the specimens with Ø30 mm holes. Figure 10 illustrates a possible shape of these air inclusions found in the Ø30 mm specimens. Mitigating measures, such as drilling an air escape channel, are planned to be implemented in future tests to ensure reliable and accurate test data.

$Ø_{hole}$	Injection material	σ_{max} (MPa)	σ_{min} (MPa)	$\Delta\sigma$ (MPa)
26	Resin	200	20	180
	Steel-reinforced resin			
	Resin	150	15	135
	Steel-reinforced resin			
	Resin	100	10	90
	Steel-reinforced resin			
30	Resin	200	20	180
	Steel-reinforced resin			
	Resin	150	15	135
	Steel-reinforced resin			
	Resin	100	10	90
	Steel-reinforced resin			

Table 1: Experimental test matrix.

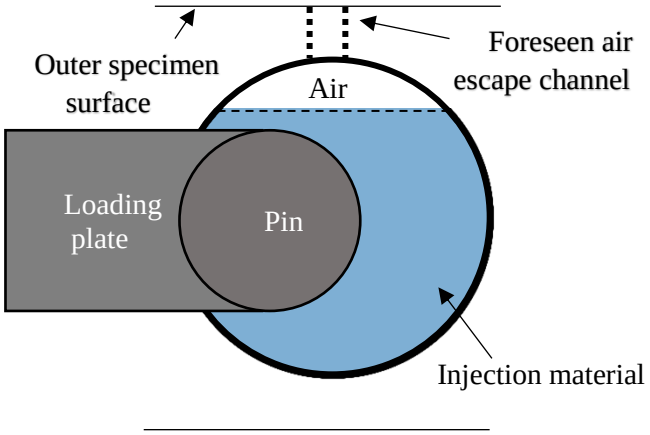

Figure 9: Air inclusions in specimens and planned mitigating measure.

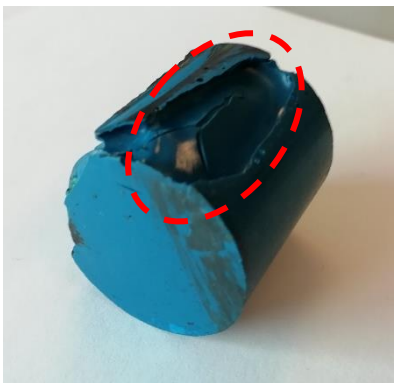

Figure 10: Example of air inclusion in actual specimen.

At the time of finalizing the paper, experiments have been carried out with resin and steel-reinforced resin with hole diameters of Ø26 and Ø30 mm with stress ranges of 90 and 180 MPa [15]. The data obtained from the Ø30 mm specimens shows significant scatter due to the air inclusions and therefore these experiments have to be redone using the proposed mitigating measures. For the specimens with Ø26 mm holes, a visual inspection of the resin infill in combination with an analysis of the quasi-static loading phase was carried out to determine the reliability of the obtained data of each experiment. Specimens with large air inclusions as well as specimens with deviating quasi-static behaviour have been disregarded [15]. Figure 11 and Figure 12 show the experimental results of the Ø26 mm specimen for the resin (R) and steel-reinforced resin (SR) subject to cyclic loads with an nominal bearing stress amplitude of 90 and 180 MPa, respectively.

Figure 11 and Figure 12 show that stabilization of the relative displacement occurs in the range of 100 000 – 200 000 cycles. In case of the 90 MPa nominal bearing stress range, the deformation of the steel-reinforced resin-injected specimen at 400 000 cycles (1 day) is 31% smaller than in case of the resin-injected specimens. After 400 000 cycles the deformation has increased by 30% compared to the initial deformation after the first cycle for both test groups. A number of tests was continued until 1.2 million applied loading cycles, after which an average increase of relative displacement was found of 4% compared to 400 000 cycles. This indicates that future tests should be designed to last for an increased number of cycles relevant for the field of application, for instance 2 million cycles in case of

bolted connections. The deformation after 400 000 cycles in case of a nominal bearing stress of 180 MPa does not significantly differ for both injection materials. It is noted that the initial, i.e. after the quasi-static loading phase, relative displacement between the loading plates is smaller in case of steel-reinforced resin injected specimens. This indicates that the steel-reinforced resin-injected specimens undergo relatively larger additional relative displacement due to cyclic loading compared to the resin-injected specimens. The deformation has increased by 250% and 150% compared to the initial deformation after the first loading cycle for the steel-reinforced resin-injected and resin-injected specimens, respectively. This difference might result from the lower Poisson's ratio of steel-reinforced resin (0.22) compared to resin itself (0.30) [13]. Due to the lower Poisson's ratio, the deviatoric stress in the steel-reinforced resin is theoretically higher, which leads to earlier onset of plastic material behaviour compared to the case of bare resin. Effects of the stress concentration in the pin-plate interface on the relative displacement between the loading plates should be studied to prevent the influence of the setup on the test results.

No generic conclusion can be drawn yet on the superiority of steel-reinforced resin compared to conventional resin in an injected bolted connection subject to cyclic loading – further research is necessary to support or reject this hypothesis. Additional experiments with a nominal bearing stress range of 135 MPa are on-going. In addition, the tests on specimens with Ø30 mm holes will be redone to exclude the influence of air inclusions. Apart from connection behaviour, also material properties are planned to be derived. It is not straightforward to derive the (steel-reinforced) resin material models on the deformation of a connection due to the relatively complicated stress conditions. Therefore, an additional set of tests is planned on uniaxially loaded cylinders of (steel-reinforced) resin under confined and unconfined conditions to allow for material modelling of the (steel-reinforced) resin under cyclic loads.

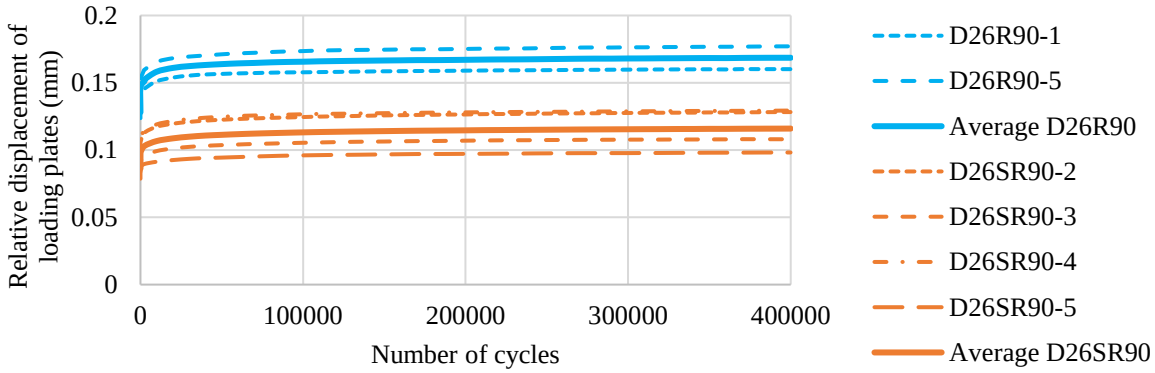

Figure 11: Relative displacement between loading plates as a function of the number of applied loading cycles at a nominal bearing stress range of 90 MPa for a specimen with Ø26 mm hole.

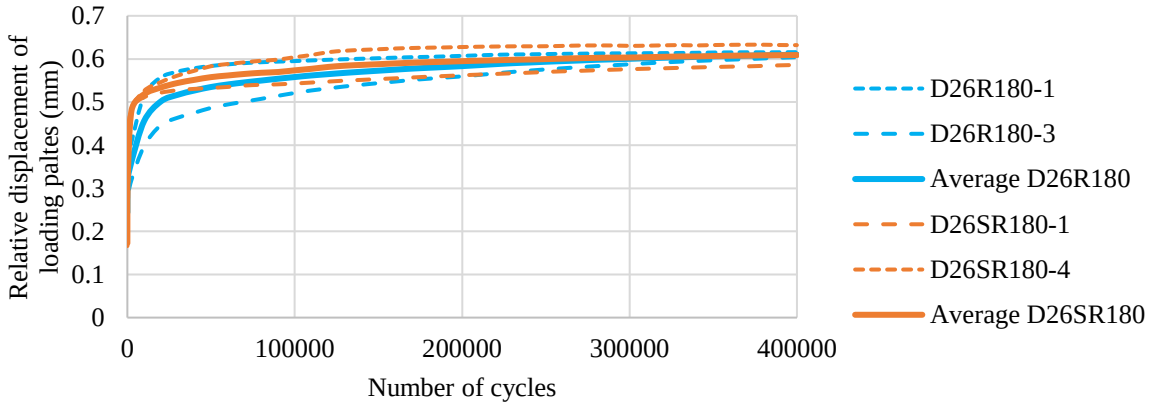

Figure 12: Relative displacement between loading plates as a function of the number of applied loading cycles at a nominal bearing stress range of 180 MPa for a specimen with Ø26 mm hole.

5 POTENTIAL APPLICATIONS FOR STEEL-REINFORCED RESINS

Generally, steel-reinforced resins can be used for purposes that aims at mitigating the effects of geometrical and dimensional deviations. The application of steel-reinforced resins is not limited to steel-to-steel [7] and steel-to-concrete [6] connections. Recently, steel-reinforced resin has also been applied in steel-to-FRP connections to obtain a shear connection in which pull-out resistance is generated by the steel-reinforced resin [16] [17].

The unevenness of bridge bearing surfaces and bridge decks can be mitigated by injecting steel-reinforced resin into the contact area, see Figure 13. An epoxy resin system is already available on the market for this purpose [18], but the use of a steel-reinforced epoxy resin system is expected to reduce costs and increase the overall connection performance. Due to the natural confinement conditions, the brittle failure mode shown in Figure 4 and Figure 6 is prevented.

Misalignment of column bases and anchor rods requires in-situ work to resolve the issue, see Figure 14. In case that the column base holes are designed as oversized, additional in-situ work (such as the enlargement of the hole in Figure 14) is prevented. After connecting the column base with the anchor rods, the bolt-hole clearance can be injected to fix the location of the column base. This design principle would allow for easy and rapid execution of the columns without doubts on connection performance.

Within demountable and reusable steel-concrete composite structures, steel-reinforced resin can be used to mitigate connection slip compared to conventional resin. Push-out tests similar to those described in EN 1994-1-1 [19] to determine the load-slip behaviour of shear connectors are on-going at Delft University of Technology [20] with the same shear connector system as used in ref. [6]. An initial FE prediction based on the material models of Xin et al. [13] shows that the initial stiffness is 36% higher in case of steel-reinforced resin compared to conventional epoxy resin. An additional set of push-out tests is on-going in which the specimens are subject to cyclic loading to determine the fatigue resistance of the demountable shear connector system.

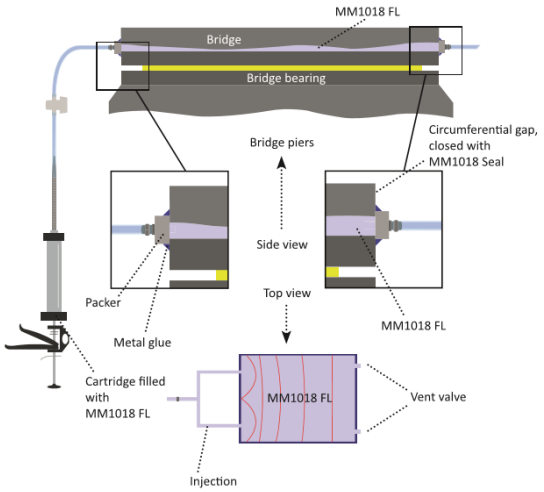

Figure 13: Injecting epoxy resin into the contact area of a bridge bearing to mitigate the unevenness of the contact surfaces [18].

Figure 14: In-situ hole cutting in the column base to ensure alignment with the anchor rods [21].

6 CONCLUSIONS

The main outcomes of the research in the field of steel-reinforced resins are as follows:

- The use of (steel-reinforced) resin in a bolted connection may be used to comply with slip-resistance requirements. In case of steel-reinforced resin significantly larger hole sizes are admissible than in case of bare resin systems. For a double-lap shear connection with M20 bolts, the connection stiffness with bolt holes of Ø32 mm injected with steel-reinforced resin was similar to that of a connection with Ø22 mm bolt holes injected with epoxy resin.
- Analytical and numerical homogenization methods have been successfully employed to

model the quasi-static behavior of steel-reinforced resins.

- Degradation of material properties of (steel-reinforced) resins due to cyclic loading leads to a decrease of the (connection) stiffness. This degradation is quantified by simple pin connection setup in which the (steel-reinforced) resin is subjected to cyclic loading. Preliminary results indicate that the deformation after 400 000 cycles in case of a Ø26 mm hole is 31% smaller for steel-reinforced resin compared to resin at a nominal bearing stress of 90 MPa. For a bearing stress of 180 MPa no significant difference between the injection materials was found. Tests at an intermediate bearing stress range of 135 MPa are on-going to determine the trend of the relative performance of resin and steel-reinforced resin under the confined conditions of a bolt hole.
- Improvements in the preparation phase of the simple pin connection specimens are necessary to avoid air inclusions in the (steel-reinforced) resin layer. These improvements are expected to reduce the scatter in the results.
- Effects of the stress concentration in the pin-plate interface on the relative displacement between the loading plates should be studied to prevent the influence of the setup on the test results. Tests on simple pin connections with a larger number of loading cycles may be necessary, depending on the field of application.
- Steel-reinforced resins can be used in applications where the effects of geometrical and dimensional imperfections must be mitigated. The steel-reinforced resin provides a continuous load path that is able to transfer external forces at a lower cost compared to conventional resin systems or other repair methods.

ACKNOWLEDGEMENTS

This research was carried out under project number T16045 in the framework of the Research Program of the Materials innovation institute (M2i) (www.m2i.nl) supported by the Dutch government.

REFERENCES

[1] NEN, EN1993-1-8 - Eurocode 3: Design of steel structures – Part 1-8: Design of Joints, Delft: NEN, 2005.

[2] A. Gresnigt and J. Stark, “Design of bolted connections with injection bolts,” in *Proceedings of the Third International Workshop - Connections in Steel Structures III*, Trento, 1996.

[3] N. Gresnigt, G. Sedlacek and M. Paschen, "Injection bolts to repair old bridges," [Online]. Available: http://citeseerx.ist.psu.edu/viewdoc/download?doi=10.1.1.552.4959&rep=rep1&type=pdf. [Accessed 14 01 2019].

[4] Rijkswaterstaat, “Eisen voor voegovergangen,” Rijkswaterstaat Steunpunt Opdrachtgeversschap, Utrecht, 2007.

[5] F. J. Wedekamper, “Avaliação de resinas epóxi para aplicação em end fittings de dutos flexíveis,” Universidade Federal do Rio Grande do Sul, Rio Grande, 2017.

[6] M. P. Nijgh, I. A. Girbacea and M. Veljkovic, “Elastic behaviour of tapered composite beam optimized for reuse,” *Engineering Structures,* vol. 183, pp. 366-374, 2019.

[7] M. P. Nijgh, “New materials for injected bolted connections – A feasibility study for demountable connections,” Delft University of Technology, Delft, 2017.

[8] NEN, EN1090-2: Execution of steel structures and aluminium structures – Part 2: technical requirements for steel structures, Delft: NEN, 2008.

[9] M. P. Nijgh, H. Xin and M. Veljkovic, “Non-linear hybrid homogenization method for steel-reinforced resin,” *Construction and Building Materials,* vol. 182, pp. 324-333, 2018.

[10] A. Reuss, “Berechnung der Fließgrenze von Mischkristallen auf Grund der Plastizitätsbedingung für Einkristalle,” *Zeitschrift für Angewandte Mathematik und Mechanik,* no. 9, pp. 49-59, 1929.

[11] J. Fish, Practical Multiscaling, John Wiley & Sons, 2013.

[12] J. Fish and R. Fan, “Mathematical homogenization of nonperiodic heterogeneous media subjected to large deformation transient loading,” *International Journal for Numerical Methods in Engeering,* vol. 76, pp. 1044-1064, 2008.

[13] H. Xin, M. P. Nijgh and M. Veljkovic, “Computational homogenization simulation on steel-reinforced resin used in the injected bolted connections,” *Composite Structures,* vol. 210, pp. 942-957, 2019.

[14] ASTM International, “D7791 - 12: Standard Test Method for Uniaxial Fatigue Properties of Plastics,” ASTM International, West Conshohocken, 2012.

[15] K. Roupakas, “Fatigue behavior of resin and steel-reinforced resin used in IBCs,” Delft University of Technology, Delft, 2019 (expected).

[16] S. Figuera, "Steel-reinforced resin joining technology," Hogeschool Rotterdam, Rotterdam, 2019.

[17] F. Csillag, “Demountable deck-to-girder connection of FRP-steel hybrid bridges,” Delft University of Technology, Delft, 2018.

[18] DIAMANT - The Metalplastic Company, “Official German General Building Approval: MM1018,” DIAMANT Metallplastic GmbH, Mönchengladbach, 2017.

[19] NEN, EN 1994-1-1 - Eurocode 4: Design of composite steel and concrete structures - Part 1-1: General rules and rules for buildings, Delft: NEN, 2005.

[20] A. Sarri, “Assessment of a steel-concrete shear connector system with resin-injected bolts,” Delft University of Technology , Delft, 2019.

[21] J. M. Fisher and L. A. Kloiber, “Field Fixes - Common problems in design, fabrication and erection: solutions and prevention,” The American Institue of Steel Construction, Chicago, 2006.